



# Preparation of porous nano-calcium titanate microspheres and its adsorption behavior for heavy metal ion in water

Dong Zhang<sup>a,\*</sup>, Chun-li Zhang<sup>b</sup>, Pin Zhou<sup>a</sup>

<sup>a</sup> School of Environmental and Chemical Engineering, Shenyang Ligong University, Shenyang 110159, PR China

<sup>b</sup> Xi zang University, Lasa 850000, PR China

## ARTICLE INFO

### Article history:

Received 25 July 2010

Received in revised form 8 November 2010

Accepted 23 November 2010

Available online 1 December 2010

### Keywords:

Template method

Porous nano-calcium titanate microspheres

Heavy metal ion

Adsorption

Kinetics

Thermodynamics

Flame atomic absorption spectrometric

## ABSTRACT

Using D311 resin as a template, porous nano-calcium titanate microspheres (PCTOM) were prepared by a citric acid complex sol-gel method and characterized by X-ray diffraction (XRD), SEM and FTIR. The method's adsorption capabilities for heavy metal ions such as lead, cadmium and zinc were studied and adsorption and elution conditions were investigated. Moreover, taking the cadmium ion as an example, the thermodynamics and kinetics of the adsorption were studied. The results show that the microspheres were porous and were made of perovskite nano-calcium titanate. The lead, cadmium and zinc ions studied could be quantitatively retained at a pH value range of 5–8. The adsorption capacities of PCTOM for lead, cadmium and zinc were found to be 141.8 mg g<sup>-1</sup>, 18.0 mg g<sup>-1</sup> and 24.4 mg g<sup>-1</sup> respectively. The adsorption behavior followed a Langmuir adsorption isotherm and a pseudo-second-order kinetic model, where adsorption was an endothermic and spontaneous physical process. The adsorbed metal ions could be completely eluted using 2 mol L<sup>-1</sup> HNO<sub>3</sub> with preconcentration factors over 100 for all studied heavy metal ions. The method has also been applied to the preconcentration and FAAS determination of trace lead, cadmium and zinc ion in water samples with satisfactory results.

© 2010 Elsevier B.V. All rights reserved.

## 1. Introduction

In recent years, heavy metal pollution of water has been a public concern. Determining the presence of heavy metals such as Pb, Cd and Zn in water is typically accomplished by atomic absorption spectrometry and inductively coupled plasma atomic emission spectrometry (ICP) [1]. However, despite continuous progress in instrumental methods for analysis, the direct determination of trace Pb, Cd and Zn in many kinds of samples is still very often difficult with these detection methods due to insufficient sensitivity and selectivity. Therefore, pretreatment steps in the analytical procedure, such as preconcentration of an analyte and/or its separation from the matrix components, are frequently necessary.

In recent years, solid-phase extraction (SPE) techniques have become increasingly popular compared with classical pre-separation and enrichment methods. SPE techniques offer high enrichment factor, rapid phase separation, low-cost and lower organic solvent consumption as well as the ability to combine with different detection techniques in on-line or off-line mode. The main solid-phase extraction sorbents are chelating resin [2,3], modified silica [4,5], active carbon [6] and carbon nanotubes [7]. Solid-phase extractions, based on nanoparticulate metal oxides such as TiO<sub>2</sub> and

Al<sub>2</sub>O<sub>3</sub>, have particularly been found to have very high enrichment capacity for separation and preconcentration of metal ions from environmental water [8–12]. Our previous studies showed that nano-barium strontium titanate and nano-calcium titanate powders are a promising solid-phase extraction adsorbent for heavy metal ions [13–18], and the results indicated that nano-barium strontium titanate and nano-calcium titanate powders have higher adsorption capacity than nanoparticulate metal oxides. However, nano-barium strontium titanate and nano-calcium titanate particles are similar to nanometer TiO<sub>2</sub> in that the particles are so small it is easy for them to coagulate and lose activity when used in adsorption of metal ions. Moreover, these titanate particles are also difficult to recover. Making the nanoparticulate into porous microspheres corrects these problems with satisfactory results [19]. However, since nano-barium strontium titanate powder is too costly, this restricts its application in practice. Compared with barium strontium titanate, calcium titanate is low-cost for preparing sources and possesses high adsorption ability for heavy metal ions [18]. But the porous nano-calcium titanate microsphere has not been studied. In this work, using D311 resin as a template, porous nano-calcium titanate microspheres were prepared by the sol-gel template method to obtain a porous microspheres adsorption agent of nano-calcium titanate (PCTOM). The adsorptive potential of PCTOM for the preconcentration of trace Pb, Cd and Zn was assessed using the batch adsorption method. Taking the cadmium ion as representative, the thermodynamics and kinetics of

\* Corresponding author.

E-mail address: [sylgdxdong@sina.com](mailto:sylgdxdong@sina.com) (D. Zhang).

the adsorption were thoroughly examined. Based on the results, the authors believe they have developed a new and effective method which uses PCTOM as the sorbent to measure preconcentration of trace Pb, Cd and Zn in water samples analyzed by flame atomic absorption spectrometry.

## 2. Experimental

### 2.1. Apparatus and reagents

X-ray diffraction (XRD) on the porous nano-calcium titanate microspheres was performed using an X' Pert Pro X-ray diffractometer (PANalytical B. V., Netherlands). Images of the D311 resin and the PCTOM were taken using an S-3400N scanning electronic microscope (Hitachi Japan) and FT-IR spectra of the resin, titanate sol-gel and the PCTOM were obtained with a WQF-410 FTIR spectrometer (Beijing No. 2 Optical Instrument Factory). The parameters for all machines were adjusted according to the manufacturer's recommendations.

A TAS-990 atomic absorption spectrometer with air-acetylene flame (Beijing Purkinjie General Instrument Co., Ltd.), equipped with deuterium background correction and lead, cadmium and zinc hollow-cathode lamps as the radiation source were used for analysis. All instrumental settings were those recommended by the manufacturer. The selected wavelengths for the determination of lead, cadmium and zinc were 283.4 nm, 228.8 nm and 213.9 nm, respectively.

The pH values were measured with a PHS-3C acidometer supplied with a combined electrode (Shanghai REX Instrument Factory, Shanghai, China).

The reagents,  $\text{Ca}(\text{NO}_3)_2$  and citric acid were analytical grade and the tetrabutyl titanate was chemically pure. The resin used was a D311 macropore weak alkali acrylic acid anion exchange resin (Anhui Sanxing Resin Technology Co., Ltd.). Stock solutions of  $\text{Pb}^{2+}$  ( $0.5 \text{ g L}^{-1}$ ),  $\text{Cd}^{2+}$  ( $0.1 \text{ g L}^{-1}$ ) and  $\text{Zn}^{2+}$  ( $0.1 \text{ g L}^{-1}$ ) were prepared by dissolving each metal (purity >99.99%) in a small amount of 1 + 1 nitric acid separately and diluting to 1000 mL with 1% nitric acid. Working standard solutions were prepared by appropriate dilution of the stock standard solutions. The water in this study was double-quartz sub-boiling distilled water.

### 2.2. Preparation of the porous nano-calcium titanate microspheres

The calcium titanate sol was prepared according to reference [18]. The D311 resin was immersed in 20% (v/v) of ethanol for a whole night, and then washed with water until there was no odor of ethanol. After drying at  $105^\circ\text{C}$ , the resin was immersed in the prepared calcium titanate sol then placed under vacuum for 30 min before being vacuum-impregnated for 12 h. After infusing, the samples were leached, and then placed on vitrolite for drying at  $105^\circ\text{C}$ . The vacuum-impregnation, leaching and drying process was repeated three times. Finally, the dried D311 resin was burned at  $650^\circ\text{C}$  for 7 h under air atmosphere and subsequently cooled to room temperature in a desiccator. The porous calcium titanate microsphere was immersed in  $2 \text{ mol L}^{-1}$   $\text{HNO}_3$  for 15 min. After washing to neutral with water, it was dried at  $105^\circ\text{C}$  and stored in a desiccator.

### 2.3. General procedure

A specific amount of heavy metal ion solution was placed into a 50 mL calibrated Erlenmeyer flask. The pH was adjusted to 6.0 with nitric acid or ammonia solution. After dilution to the mark with water, 0.1 g of PCTOM was added. Covered with a plug, the Erlenmeyer flask was shaken for 40 min in a constant temperature

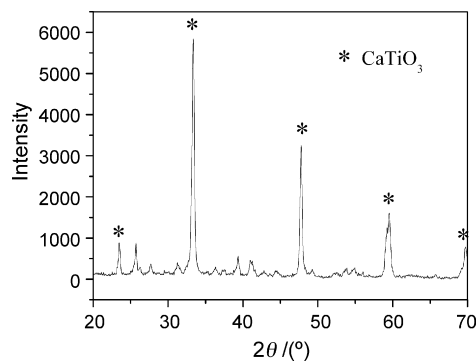


Fig. 1. XRD pattern of porous nano-calcium titanate microspheres.

bath shaker (Jintan Experiment Instrument Factory, Jiangsu China). The supernatant fluid was then directly aspirated into the atomic absorption spectrometer, where the concentrations of  $\text{Pb}^{2+}$ ,  $\text{Cd}^{2+}$  or  $\text{Zn}^{2+}$  were determined by FAAS and absorption capacity was calculated. Then the PCTOM was washed with water and the adsorbed metal ions were eluted with 5 mL of  $2 \text{ mol L}^{-1}$   $\text{HNO}_3$  solution by shaking for 5 min. The concentrations of the metal ions in the eluents were determined by FAAS. Recoveries were calculated from concentrations of supernatants and eluents.

## 3. Results and discussion

### 3.1. Characterization of the porous nano-calcium titanate microsphere

The diffraction pattern of the porous nano-calcium titanate microspheres characterized using XRD is shown in Fig. 1. The sharp peaks of the crystal structure at 23.48, 33.36, 47.76, 59.54, and 69.76 can be attributed to  $\text{CaTiO}_3$  [18]. Based on these peaks, the calcium titanate sample had a perovskite structure. According to the expression of Scherrer, the average crystal diameter is 26 nm [13].

The SEM images of the D311 macropore weak alkali acrylic acid anion exchange resin, both before and after being immersed in the calcium titanate sol-gel, and resulting PCTOM, are shown in Fig. 2. The SEM images show that the sample is a porous microsphere and is made up of small particulates.

Fig. 3 provides the FT-IR spectra of the resin, calcium titanate sol-gel and PCTOM samples. The spectra for the resin shows (spectral line 1): absorption peaks at  $3459 \text{ cm}^{-1}$  and  $3302 \text{ cm}^{-1}$ , indicating N–H and O–H bond stretching due to functional groups of the resin; the presence of bands at  $3087 \text{ cm}^{-1}$  and  $1572\text{--}1450 \text{ cm}^{-1}$  that correspond to aromatic structures; and peaks at  $2947 \text{ cm}^{-1}$  and  $2841 \text{ cm}^{-1}$  attributed to methyl and methylene groups. The vibration of acid amides appearing at  $1660 \text{ cm}^{-1}$  and adsorption peaks around  $1444 \text{ cm}^{-1}$ ,  $1300 \text{ cm}^{-1}$  and  $1122 \text{ cm}^{-1}$  could be due to the bending vibration of C–H and C–N bonds [19,20]. Spectral line 2 of Fig. 3 shows the IR spectrum for the calcium titanate sol-gel, where the following bands were identified:  $3419 \text{ cm}^{-1}$  and  $1635 \text{ cm}^{-1}$  (hydroxyl group);  $3200 \text{ cm}^{-1}$ ,  $1545 \text{ cm}^{-1}$  and  $1415 \text{ cm}^{-1}$  (carboxylic group);  $2949 \text{ cm}^{-1}$  and  $2889 \text{ cm}^{-1}$  (methylene and methyl groups);  $1385 \text{ cm}^{-1}$  (bands of N–O due to nitrate);  $1082 \text{ cm}^{-1}$  (C–O–Ti);  $1049 \text{ cm}^{-1}$  (C–O–Ca); and  $552 \text{ cm}^{-1}$  (Ti–O). After the resin was macerated with the calcium titanate sol-gel, the characteristic peaks for calcium titanate sol-gel appeared on the spectra. The stretching and bending vibration of O–H also appeared at  $3396 \text{ cm}^{-1}$  and  $1643 \text{ cm}^{-1}$ . The C–H stretching vibrations shifted to  $3030 \text{ cm}^{-1}$ ,  $2931 \text{ cm}^{-1}$  and  $2721 \text{ cm}^{-1}$ , indicating that the calcium titanate sol-gel loaded on the resin interacted with the functional groups of the resin

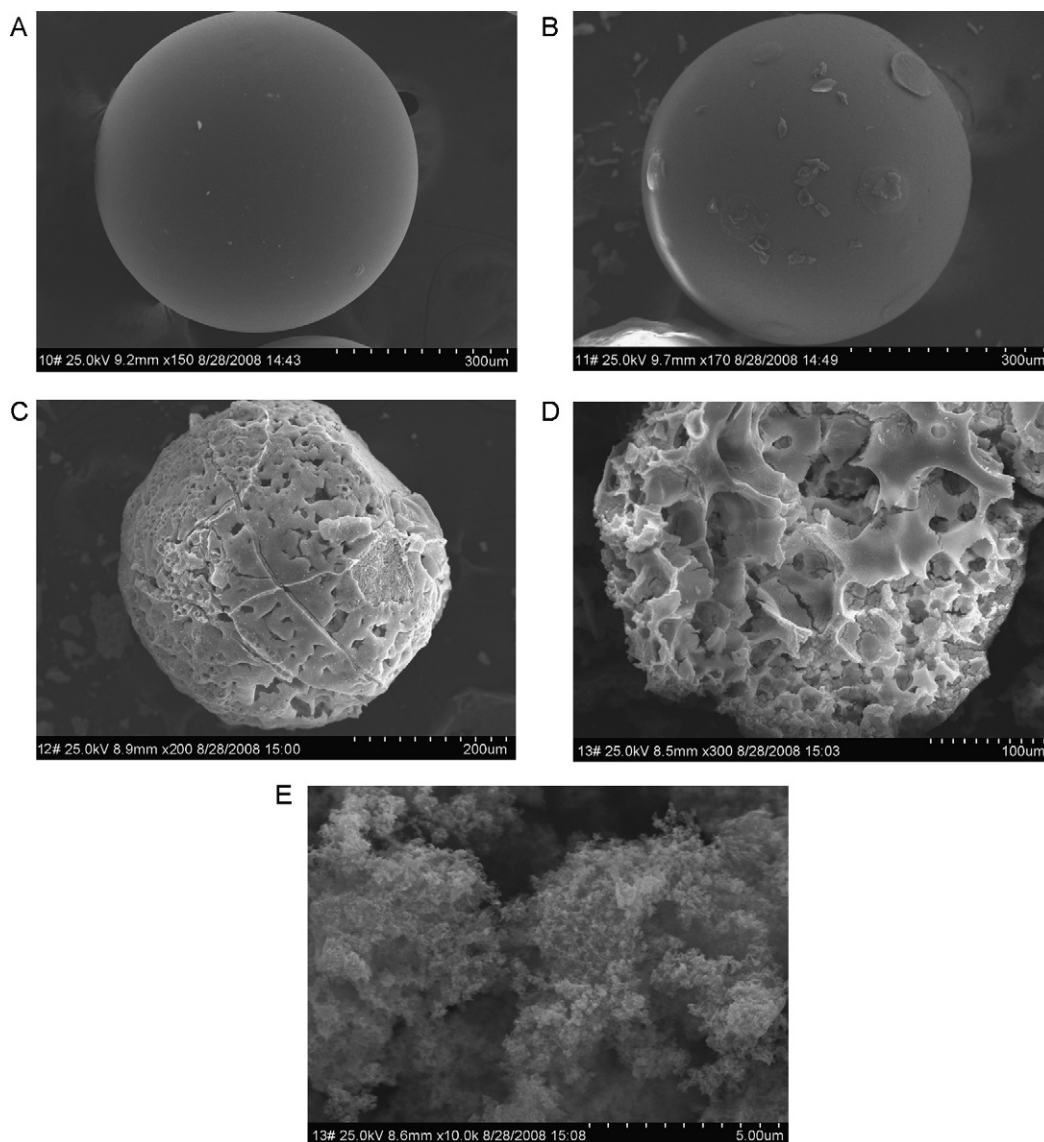


**Fig. 2.** (A) SEM micrographs of D311 rosin. (B) SEM micrographs of the rosin macerated by CTO sol. (C) SEM micrographs of the panorama of PCTOM. (D) SEM micrographs of the section of PCTOM ( $\times 300$ ). (E) SEM micrographs of the section of PCTOM ( $\times 10000$ ).

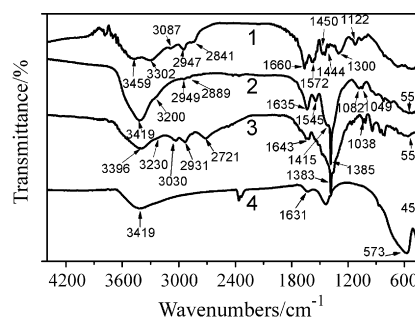
already in place. After being calcined at  $650^{\circ}\text{C}$ , the spectra peaks for the resin and calcium titanate sol–gel samples disappeared. Additionally, the stretching and bending vibration of Ca–Ti–O appeared at  $573\text{ cm}^{-1}$  and  $453\text{ cm}^{-1}$ , indicating the presence of calcium titanate. Two absorption peaks appeared near  $3419\text{ cm}^{-1}$  and  $1631\text{ cm}^{-1}$ , caused by the stretching and bending vibration of the O–H bonds due to the  $\text{CaTiO}_3$  surface [18].

### 3.2. Static adsorption experiments

#### 3.2.1. Effect of pH

Our previous studies show that the pH value of a solution plays an important role with respect to the adsorption of different ions on titanate surfaces [15,18], as the pH affects the distribution of active sites on the titanate surface. The pH affects the distribution of active sites on a titanate surface. At high pH, the  $\text{OH}^-$  on the surface provides the higher potential of binding cations. The decrease of pH leads to lower  $\text{OH}^-$  concentration on the surface, so the adsorption of cations onto calcium titanate decreases accordingly. To evaluate the pH effect, the pH value of sample solutions was adjusted from 1 to 8. The results are shown in Fig. 4. The adsorption percent-

ages of  $\text{Pb}^{2+}$ ,  $\text{Cd}^{2+}$  and  $\text{Zn}^{2+}$  on the PCTOM were dependent on the pH value of the medium. Increasing the pH resulted in an increase of amount adsorbed. The adsorptions of  $\text{Pb}^{2+}$  and  $\text{Cd}^{2+}$  at the pH range of 4–8, and of  $\text{Zn}^{2+}$  at the pH range of 5–8, were over 95%. To preconcentrate  $\text{Pb}^{2+}$ ,  $\text{Cd}^{2+}$  and  $\text{Zn}^{2+}$  simultaneously, and to avoid



1-D311 rosin; 2-CTO gel; 3-the rosin macerated by CTO sol; 4-PCTOM

**Fig. 3.** FT-IR spectrograms: (1) D311 rosin; (2) CTO gel; (3) the rosin macerated by CTO sol; (4) PCTOM.

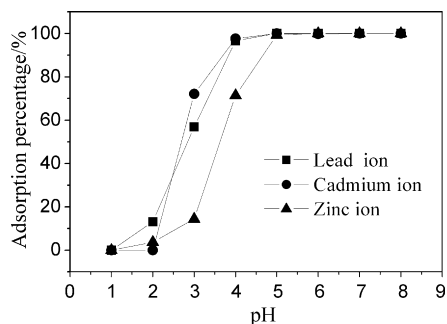


Fig. 4. Effect of pH on the adsorption  $Pb^{2+}$ : 2.0 mg,  $Cd^{2+}$ : 0.5 mg,  $Zn^{2+}$ : 0.5 mg, and sample volume: 50 mL.

the precipitation of metal ions at high concentration, pH 6.0 was selected as the optimal pH condition.

### 3.2.2. The effect of contact time

At a pH of 6.0, the adsorption capacities for  $Pb^{2+}$ ,  $Cd^{2+}$  and  $Zn^{2+}$  were determined with different shaking times (Fig. 5). The results indicate that the amount adsorbed increased with an increase in shaking time and reached equilibrium at 30 min for  $Pb^{2+}$  and  $Cd^{2+}$ , and 15 min for  $Zn^{2+}$ . Therefore, the shaking time was set to 40 min for this study.

### 3.3. Adsorption isotherms and thermodynamic Studies

Heavy metal ion adsorption isotherm data starting at different initial concentrations were investigated following the models of Langmuir and Freundlich. In this paper, the thermodynamics of the adsorption were studied using the cadmium ion, where  $Cd^{2+}$  concentration had reached equilibrium.

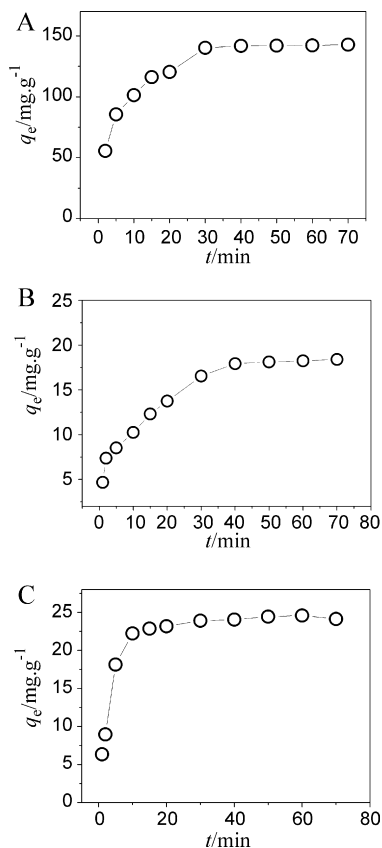


Fig. 5. (A) Effect of contact time on adsorption of lead ion. (B) Effect of contact time on adsorption of cadmium ion. (C) Effect of contact time on adsorption of zinc ion.

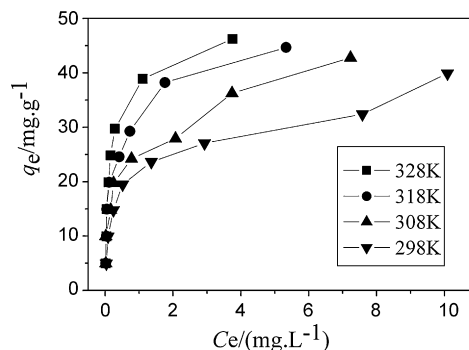


Fig. 6. Adsorption isotherms under different temperatures.

The expression of the Langmuir model is [18]

$$\frac{C_e}{q_e} = \frac{1}{K_L q_m} + \frac{C_e}{q_m} \quad (1)$$

where  $q_e$  is the equilibrium metal ion concentration on the adsorbent ( $mg\ g^{-1}$ ),  $C_e$  is the equilibrium metal ion concentration in solution ( $mg\ L^{-1}$ ),  $q_m$  is the monolayer capacity of the adsorbent ( $mg\ g^{-1}$ ) and  $K_L$  is the Langmuir adsorption constant ( $L\ mg^{-1}$ ). A plot of  $C_e/q_e$  vs.  $C_e$  gives a straight line of slope  $1/q_m$  and intercept,  $1/(q_m K_L)$ . The Langmuir equation is applicable to homogeneous sorption, where the sorption of each sorbate molecule onto the surface has equal sorption activation energy.

The logarithmic expression of the Freundlich equation is [18]

$$\ln q_e = \ln K_F + \frac{1}{n} \ln C_e \quad (2)$$

where  $q_e$  is the equilibrium metal ion concentration on the adsorbent ( $mg\ g^{-1}$ ),  $C_e$  is the equilibrium metal ion concentration in solution ( $mg\ L^{-1}$ ), and  $K_F$  ( $L\ mg^{-1}$ ) and  $n$  are the Freundlich constants for adsorption capacity and adsorption intensity, respectively, and which are characteristics of the system. The Freundlich equation is employed to describe heterogeneous systems and reversible adsorption and is not restricted to the formation of monolayers. From the plot of  $\ln q_e$  vs.  $\ln C_e$  for the adsorption of cadmium onto GPCTO, one can get the intercept value of  $K_F$  and the slope of  $1/n$ .

The adsorption isotherms at various temperatures are shown in Fig. 6. The values of  $q_m$ ,  $K_L$ ,  $K_F$ , and  $1/n$  and the correlation coefficients ( $r$ ) for Langmuir and Freundlich are given in Table 1.

The values of the correlation coefficients demonstrate almost perfect agreement between the experimental data and the Langmuir model. This suggests that the adsorption of  $Cd^{2+}$  by the PCTOM was monolayer-type, which agrees with the general observation that the adsorption from an aqueous solution usually forms a layer on the adsorbent surface. The values of the Langmuir constant,  $K_L$ , increased as temperature increased, indicating that the adsorption capacity and intensity of adsorption are enhanced at higher temperatures.

Thermodynamic parameters such as isothermic adsorption enthalpy ( $\Delta H$ ), Gibbs free energy ( $\Delta G$ ) and entropy ( $\Delta S$ ) for the adsorption process can be calculated from the van't Hoff equation

Table 1  
The parameter of Langmuir and Freundlich isotherms equations.

| T (K) | Langmuir constants |       |       | Freundlich constants |       |       |
|-------|--------------------|-------|-------|----------------------|-------|-------|
|       | $q_m$              | $K_L$ | $r^2$ | $n$                  | $K_F$ | $r^2$ |
| 298   | 38.760             | 1.709 | 0.977 | 3.127                | 0.198 | 0.993 |
| 308   | 43.103             | 2.442 | 0.979 | 3.319                | 0.247 | 0.921 |
| 318   | 45.872             | 4.449 | 0.995 | 2.954                | 0.313 | 0.889 |
| 328   | 47.393             | 5.703 | 0.999 | 2.667                | 0.382 | 0.860 |



**Table 2**  
Thermodynamic parameters of Cd<sup>2+</sup> adsorption on PCTOM.

| Temperature (K) | $\Delta H$ (kJ mol <sup>-1</sup> ) | $\Delta G$ (kJ mol <sup>-1</sup> ) | $\Delta S$ (J mol <sup>-1</sup> K <sup>-1</sup> ) |
|-----------------|------------------------------------|------------------------------------|---|
| 298             | 39.864                             | -1.327                             | 138.225   |
| 308             |                                    | -2.286                             | 136.852   |
| 318             |                                    | -3.946                             | 137.768   |
| 328             |                                    | -4.748                             | 136.011   |

and Gibbs–Helmholtz equation [18,21]

$$\ln C_e = -\ln K_0 + \frac{\Delta H}{RT} \quad (3)$$

$$\Delta G = -RT \ln C_e \quad (4)$$

$$\Delta S = \frac{\Delta H - \Delta G}{T} \quad (5)$$

where  $R$  is the ideal gas constant (8.314 J mol<sup>-1</sup> K<sup>-1</sup>),  $T$  is temperature (K),  $K_0$  is constant and  $C_e$  is the solution concentration at equilibrium. The slope of the plots of  $\ln C_e$  versus  $1/T$  used to determine  $\Delta H$ ,  $\Delta G$  and  $\Delta S$  were obtained from Eq. (4) and (5) respectively. The results are listed in Table 2.

In fact, the positive value of enthalpy change  $\Delta H$  for the processes further confirms the endothermic nature of the process; the free energy,  $\Delta G$ , is negative at all temperatures and decreases as temperature rises. This suggests the adsorption process is spontaneous and the spontaneity increases as temperature increases. The positive entropy of adsorption reflects the affinity of the adsorbent material toward Cd<sup>2+</sup>; it is the solvent effect of substitution [18,21].

### 3.4. Kinetics modeling

In order to quantify the extent of uptake in adsorption kinetics, two simple kinetic models were tested. Lagergren's first-order rate equation [18,21] based on solid capacity is generally expressed as

$$\ln(q_e - q_t) = \ln q_e - K_1 t \quad (6)$$

where  $K_1$  (min<sup>-1</sup>) is the equilibrium rate constant of the pseudo-first-order adsorption, and  $q_e$  and  $q_t$  (mg g<sup>-1</sup>) are the amounts of metal ions adsorbed at equilibrium at any time  $t$ .

A pseudo-second-order adsorption kinetic rate equation is

$$\frac{t}{q_t} = \frac{1}{K_2 q_e^2} + \frac{t}{q_e} \quad (7)$$

where  $K_2$  (g·(mg min)<sup>-1</sup>) is the rate constant of the pseudo-second-order adsorption.

According to the data in Fig. 7, the values of  $k_1$ ,  $k_2$ , and  $q_e$  can be obtained from the intercept and slope of the plot of  $(\ln(q_e - q_t))$  versus  $t$  and  $(t/q_t)$  versus  $t$ , respectively.

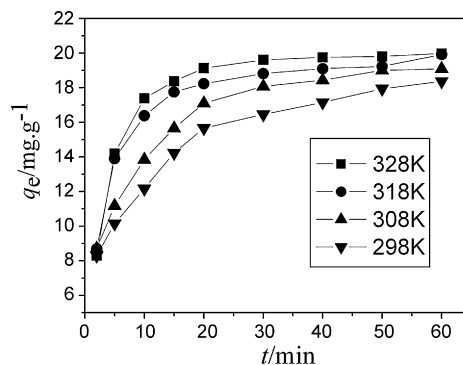
The results fit the pseudo-second-order plot model better than they fit Lagergren's first-order rate equation, with all  $r^2$  values greater than 0.999.

The activation energy for Cd(II) adsorption onto the PCTOM was calculated by using the Arrhenius equation

$$K_2 = K_0 e^{-\frac{E_a}{RT}} \quad (8)$$

**Table 3**Preconcentration and recoveries of Pb<sup>2+</sup>, Cd<sup>2+</sup> and Zn<sup>2+</sup>.

| Volume of the solution (mL) | The quantity in eluent (μg) |                  |                  | Recovery (%)     |                  |                  | Enrichment factor |
|-----------------------------|-----------------------------|------------------|------------------|------------------|------------------|------------------|-------------------|
|                             | Pb <sup>2+</sup>            | Cd <sup>2+</sup> | Zn <sup>2+</sup> | Pb <sup>2+</sup> | Cd <sup>2+</sup> | Zn <sup>2+</sup> |                   |
| 50                          | 10.25                       | 0.971            | 1.98             | 102.5            | 97.1             | 99.5             | 10                |
| 100                         | 9.91                        | 1.030            | 1.93             | 99.1             | 103.0            | 96.5             | 20                |
| 150                         | 10.43                       | 0.959            | 2.01             | 104.3            | 95.9             | 100.5            | 30                |
| 200                         | 9.68                        | 0.961            | 1.96             | 96.8             | 96.1             | 98.0             | 40                |
| 250                         | 9.72                        | 0.950            | 1.90             | 97.2             | 95.0             | 95.0             | 50                |
| 500                         | 9.47                        | 0.902            | 1.84             | 94.7             | 90.2             | 92.0             | 100               |

**Fig. 7.** Effect of time on adsorption at various temperatures.

and the equation may be linearized by taking logarithms

$$\ln K_2 = \ln K_0 - \frac{E_a}{R} \times \frac{1}{T} \quad (9)$$

here,  $K_2$  is the rate constant of the pseudo-second-order adsorption kinetic rate temperature  $T$  (K),  $K_0$  is the frequency factor,  $R$  is the ideal gas constant (8.314 J·(mol K)<sup>-1</sup>), and  $E_a$  (kJ mol<sup>-1</sup>) is the activation energy for the adsorption process. The magnitude of the activation energy can indicate the type of sorption.

The activation energy was obtained from the slope of the plot of  $\ln K_2$  values versus  $1/T$  using Eq. (10) and was found to be 20.991 kJ mol<sup>-1</sup>.

$$\ln K_2 = -2524.8 \frac{1}{T} + 3.8987 \quad (R^2 = 0.964) \quad (10)$$

For adsorption with an activation energy of less than 40 kJ mol<sup>-1</sup>, the main interaction between the metal ion and the PCTOM is probably physisorption [18,21].

### 3.5. Elution conditions

The result in Fig. 4 shows that the adsorption of cations at pH < 1 could be negligible. For this reason, after the heavy metal ions were adsorbed under the optimized adsorption conditions, 5 mL of HNO<sub>3</sub> (0.01–5.0 mol L<sup>-1</sup>) were used for elution for 5 min. The recovery results showed that recovery increased with an increase of HNO<sub>3</sub> concentration. When the concentration of HNO<sub>3</sub> was higher than 1.0 mol L<sup>-1</sup>, all the recoveries were up to 95% for Pb<sup>2+</sup>, Cd<sup>2+</sup> and Zn<sup>2+</sup>. Therefore, for sufficient elution, 2.0 mol L<sup>-1</sup> HNO<sub>3</sub> was chosen. After elution, the PCTOM was dried and reused 10 times. Its adsorption performance did not decrease, indicating that this adsorption agent was very stable.

### 3.6. Static adsorption capacity

From Fig. 5, the static adsorption capacities of PCTOM to Pb<sup>2+</sup>, Cd<sup>2+</sup> and Zn<sup>2+</sup> at room temperature were 141.8 mg g<sup>-1</sup>, 18.0 mg g<sup>-1</sup> and 24.4 mg g<sup>-1</sup>, respectively.

**Table 4**  
Determination of Pb<sup>2+</sup>, Cd<sup>2+</sup> and Zn<sup>2+</sup> in water samples (n=6).

| Samples of water | Added ( $\mu\text{g L}^{-1}$ ) |                  |                  | Found ( $\mu\text{g L}^{-1}$ ) |                  |                  | Recovery (%)     |                  |                  |
|------------------|--------------------------------|------------------|------------------|--------------------------------|------------------|------------------|------------------|------------------|------------------|
|                  | Pb <sup>2+</sup>               | Cd <sup>2+</sup> | Zn <sup>2+</sup> | Pb <sup>2+</sup>               | Cd <sup>2+</sup> | Zn <sup>2+</sup> | Pb <sup>2+</sup> | Cd <sup>2+</sup> | Zn <sup>2+</sup> |
| Tap water        | 0                              | 0                | 0                | 5.32                           | 0                | 9.60             | –                | –                | –                |
|                  | 5.00                           | 2.00             | 5.00             | 10.41                          | 1.91             | 14.31            | 101.8            | 95.5             | 94.2             |
|                  | 10.00                          | 5.00             | 10.00            | 15.19                          | 4.82             | 20.00            | 98.7             | 96.4             | 104.0            |
| River water      | 0                              | 0                | 0                | 22.30                          | 11.45            | 24.70            | –                | –                | –                |
|                  | 10.00                          | 5.00             | 10.00            | 32.06                          | 21.37            | 34.20            | 97.6             | 99.2             | 95.0             |
|                  | 20.00                          | 10.00            | 20.00            | 41.18                          | 30.83            | 44.12            | 94.4             | 96.9             | 97.1             |

### 3.7. Enrichment factor and detection limits

In order to explore the possibility of enriching low concentrations of analytes from large volumes, the effect of sample volume on the retention of heavy metal ions was also investigated. For this purpose, 10  $\mu\text{g}$  of Pb<sup>2+</sup>, 1  $\mu\text{g}$  of Cd<sup>2+</sup> and 2  $\mu\text{g}$  of Zn<sup>2+</sup> were dissolved together in various volumes of water. After adsorption, the samples were eluted with 5 mL of elution liquid. The amounts recovered are listed in Table 3.

When the solution volume was 500 mL, the recoveries were above 90% and the enrichment factor was 100. The detection limits were calculated using the concentration of three times standard deviation, calculated from 11 runs of the blank solution with concentrations of Pb<sup>2+</sup>, Cd<sup>2+</sup> and Zn<sup>2+</sup> at 0.072  $\mu\text{g L}^{-1}$ , 0.0083  $\mu\text{g L}^{-1}$  and 0.014  $\mu\text{g L}^{-1}$ , respectively. The relative standard deviations (RSD) for Pb<sup>2+</sup>, Cd<sup>2+</sup> and Zn<sup>2+</sup> were 3.4%, 2.8% and 4.2%, respectively (n = 11, C<sub>Pb</sub> = 100  $\mu\text{g L}^{-1}$ , C<sub>Cd</sub> = C<sub>Zn</sub> = 10  $\mu\text{g L}^{-1}$ ).

### 3.8. Effects of interference ions

Various interference ions were added into a 50 mL volumetric flask containing 10  $\mu\text{g}$  of Pb<sup>2+</sup> and 5  $\mu\text{g}$  of Cd<sup>2+</sup> and Zn<sup>2+</sup> to investigate the effects of common coexisting ions on the adsorption of Pb<sup>2+</sup>, Cd<sup>2+</sup> and Zn<sup>2+</sup>. The experimental results show that recovery of the target analytes remained above 95% even in the presence of ions in the following concentrations: 100 mg for Na<sup>+</sup>, K<sup>+</sup>, NH<sub>4</sub><sup>+</sup> and NO<sub>3</sub><sup>-</sup>; 50 mg for Ca<sup>2+</sup> and Mg<sup>2+</sup>; 20 mg for Al<sup>3+</sup>, PO<sub>4</sub><sup>3-</sup>, Cr(VI) and Cl<sup>-</sup>; 10 mg for Cr(III), Ag<sup>+</sup>, Co<sup>2+</sup>, Ni<sup>2+</sup> and Cu<sup>2+</sup>; and 5 mg for Fe<sup>3+</sup>. The results indicate that the method has a good tolerance to matrix interference.

### 3.9. Analytical application

The proposed method was applied to the determination of Pb<sup>2+</sup>, Cd<sup>2+</sup> and Zn<sup>2+</sup> in a natural river water sample (Hun-he River, Shenyang, China) and a tap water sample collected from the water supply of Shenyang city. The water samples were filtered through a 0.45  $\mu\text{m}$  membrane filter and analyzed immediately. The analytical results and the associated recovery are given in Table 4.

The recoveries were 94.4–101.8% for Pb, 95.5–99.2% for Cd and 94.2–104.0% for Zn, which are excellent for trace analysis.

## 4. Conclusions

In this work, porous nano-calcium titanate microspheres (PCTOM) were successfully prepared by a citric acid complex sol-gel template method, and used for lead, cadmium and zinc ion adsorption and enrichment. The adsorption followed the Langmuir sorption isotherms very well and the dynamic data fit the pseudo-second-order kinetic model. The adsorbed lead, cadmium and zinc ions were eluted completely with 2 mol L<sup>-1</sup> of HNO<sub>3</sub>, which provided concentration factors of up to 100. The method was applied to the preconcentration and FAAS determination of trace lead, cadmium and zinc ions in water samples with satisfactory results and

the adsorbent can be used for at least 10 adsorption–elution cycles without observable change in performance. Based on these characteristics, the authors believe the proposed method can be effective for determining trace lead, cadmium and zinc ions in a variety of water samples.

## References

- [1] State Environmental Protection Administration of China, Analysis Method of Water and Waste Water, fourth ed., China Environmental Science Press, Inc., Beijing, 2002, pp. 286–415.
- [2] V.K. Jain, H.C. Mandalia, H.S. Gupte, D.J. Vyas, Azocalix[4]pyrrole Amberlite XAD-2: New polymeric chelating resins for the extraction, preconcentration and sequential separation of Cu(II), Zn(II) and Cd(II) in natural water samples, *Talanta* 79 (2009) 1331–1340.
- [3] Ş. Tokalıoğlu, V. Yılmaz, Ş. Kartal, A. Delibaş, C. Soykan, Synthesis of a novel chelating resin and its use for selective separation and preconcentration of some trace metals in water samples, *J. Hazard. Mater.* 169 (2009) 593–598.
- [4] F.Z. Xie, X.C. Lin, X.P. Wu, Z.H. Xie, Solid phase extraction of lead (II), copper (II), cadmium (II) and nickel (II) using gallic acid-modified silica gel prior to determination by flame atomic absorption spectrometry, *Talanta* 74 (2008) 836–843.
- [5] L.J. Zhang, X.J. Chang, Y.H. Zhai, Q. He, X.P. Huang, Z. Hu, N. Jiang, Selective solid phase extraction of trace Sc(III) from environmental samples using silica gel modified with 4-(2-morinyldiazenyl)-N-(3-(trimethylsilyl)propyl)benzamide, *Anal. Chim. Acta* 629 (2008) 84–91.
- [6] R. Gao, Z. Hu, X.J. Chang, Q. He, L.J. Zhang, Z.F. Tu, J.P. Shi, Chemically modified activated carbon with 1-acylthiosemicarbazide for selective solid-phase extraction and preconcentration of trace Cu(II), Hg(II) and Pb(II) from water samples, *J. Hazard. Mater.* 172 (2009) 324–329.
- [7] A. Duran, M. Tuzen, M. Soylak, Preconcentration of some trace elements via using multiwalled carbon nanotubes as solid phase extraction adsorbent, *J. Hazard. Mater.* 169 (2009) 466–471.
- [8] Q.X. Zhou, X.N. Zhao, J.P. Xiao, Preconcentration of nickel and cadmium by TiO<sub>2</sub> nanotubes as solid-phase extraction adsorbents coupled with flame atomic absorption spectrometry, *Talanta* 77 (2009) 1774–1777.
- [9] Y. Liu, P. Liang, L. Guo, Nanometer titanium dioxide immobilized on silica gel as sorbent for preconcentration of metal ions prior to their determination by inductively coupled plasma atomic emission spectrometry, *Talanta* 68 (2005) 25–30.
- [10] J. Yin, Z.C. Jiang, G. Chang, B. Hu, Simultaneous on-line preconcentration and determination of trace metals in environmental samples by flow injection combined with inductively coupled plasma mass spectrometry using a nanometer-sized alumina packed micro-column, *Anal. Chim. Acta* 540 (2005) 333–339.
- [11] P. Liang, Y.C. Qin, B. Hu, T.Y. Peng, Z.C. Jiang, Nanometer-size titanium dioxide microcolumn on-line preconcentration of trace metals and their determination by inductively coupled plasma atomic emission spectrometry in water, *Anal. Chim. Acta* 440 (2001) 207–213.
- [12] C.Z. Hang, B. Hu, Z.C. Jiang, N. Zhang, Simultaneous on-line preconcentration and determination of trace metals in environmental samples using a modified nanometer-sized alumina packed micro-column by flow injection combined with ICP-OES, *Talanta* 71 (2007) 1239–1245.
- [13] H.D. Su, D. Zhang, Preparation of nanometer-sized BST powder and its adsorption behavior for cadmium ion, *J. Chem. Ind. Eng.* 57 (2006) 2892–2896.
- [14] D. Zhang, H.D. Su, H. Gao, Preparation of barium–strontium titanate nanopowder and its adsorption properties for chromium(VI) and chromium(III), *Metal. Anal.* 27 (2007) 7–10.
- [15] D. Zhang, H.D. Su, H. Gao, Study on adsorption behavior of nanosized barium–strontium titanate powder for lead ion in water using FAAS, *Spectrosc. Anal.* 28 (2008) 218–221.
- [16] D. Zhang, H.D. Su, H. Gao, J.C. Liu, Adsorption behavior of barium–strontium titanate powder coated by dithizone for lead ion in water, *Acta Chim. Sinica* 65 (2007) 2549–2554.
- [17] D. Zhang, H.D. Su, H. Gao, Study on the adsorption capability of barium–strontium titanate powder coated with dithizone for cadmium ion in water, *Spectrosc. Anal.* 28 (2008) 693–696.

- [18] D. Zhang, P. Hou, Preparation of nano-calcium titanate powder and its adsorption behavior for lead ion and cadmium ion in water, *Acta Chim. Sinica* 67 (2009) 1336–1342.
- [19] D. Zhang, N. Li, D. Gao, Determination of lead and cadmium in water by flame atomic absorption spectrometry after separation/pre-concentration with manual-controlled injection porous nano-barium–strontium titanate microspheres separator, *Chin. J. Anal. Chem.* 37 (2009) 1188–1192.
- [20] J.G. Wu, *FTIR Technology and Applications in Recent Years*, vol. 4, Science and Technology Literature Press, Beijing, 1994, pp. 267–273.
- [21] D. Zhang, W.J. Zhang, X. Guan, H. Gao, H.B. He, Adsorption behavior of immobilized nanometer barium–strontium titanate for cadmium ion in water, *Spectrosc. Spectrom. Anal.* 29 (2009) 824–828.